



Water-table and discharge changes associated with the 2016–2017 seismic sequence in central Italy: hydrogeological data and a conceptual model for fractured carbonate aquifers

Marco Petitta^{1,2} · Lucia Mastrorillo³ · Elisabetta Preziosi² · Francesca Banzato¹ · Marino Domenico Barberio¹ · Andrea Billi⁴ · Costanza Cambi⁵ · Gaetano De Luca⁶ · Giuseppe Di Carlo⁷ · Diego Di Curzio⁸ · Cristina Di Salvo⁹ · Torquato Nanni¹⁰ · Stefano Palpacelli¹⁰ · Sergio Rusi⁸ · Michele Saroli¹¹ · Marco Tallini¹² · Alberto Tazioli¹⁰ · Daniela Valigi⁵ · Paola Vivalda¹⁰ · Carlo Doglioni¹

Received: 17 July 2017 / Accepted: 22 December 2017 / Published online: 24 January 2018
© The Author(s) 2018. This article is an open access publication

Abstract

A seismic sequence in central Italy from August 2016 to January 2017 affected groundwater dynamics in fractured carbonate aquifers. Changes in spring discharge, water-table position, and streamflow were recorded for several months following nine Mw 5.0–6.5 seismic events. Data from 22 measurement sites, located within 100 km of the epicentral zones, were analyzed. The intensity of the induced changes were correlated with seismic magnitude and distance to epicenters. The additional post-seismic discharge from rivers and springs was found to be higher than 9 m³/s, totaling more than 0.1 km³ of groundwater release over 6 months. This huge and unexpected contribution increased streamflow in narrow mountainous valleys to previously unmeasured peak values. Analogously to the L'Aquila 2009 post-earthquake phenomenon, these hydrogeological changes might reflect an increase of bulk hydraulic conductivity at the aquifer scale, which would increase hydraulic heads in the discharge zones and lower them in some recharge areas. The observed changes may also be partly due to other mechanisms, such as shaking and/or squeezing effects related to intense subsidence in the core of the affected area, where effects had maximum extent, or breaching of hydraulic barriers.

Keywords Earthquake · Groundwater monitoring · Italy · Co-seismic effects · Carbonate rocks

✉ Elisabetta Preziosi
elisabetta.preziosi@cnr.it

¹ Department of Earth Sciences, Sapienza University of Rome, P.le A. Moro 5, 00185 Rome, Italy

² Water Research Institute, National Research Council, Via Salaria km 29,300, PB 10, 00015 Monterotondo (Rome), Italy

³ Department of Sciences, University of Roma Tre, L.go San Leonardo Murialdo 1, 00146 Rome, Italy

⁴ Institute of Environmental Geology and Geoengineering, National Research Council, at Sapienza University of Rome, Department of Earth Sciences, P.le A. Moro 5, 00185 Rome, Italy

⁵ Department of Physics and Geology, University of Perugia, Via A. Pascoli snc, 06123 Perugia, Italy

⁶ Centro Nazionale Terremoti, Istituto Nazionale di Geofisica e Vulcanologia, Rome, Italy

⁷ Laboratori Nazionali del Gran Sasso, Istituto Nazionale di Fisica Nucleare, Via G. Acitelli, 22, 67100 Assergi (AQ), Italy

⁸ Dipartimento InGeo, Università “G. d’Annunzio”, via dei Vestini 30, 66013 Chieti, Italy

⁹ Institute of Environmental Geology and Geoengineering, National Research Council, Via Salaria km 29,300, PB 10, 00015 Monterotondo (Rome), Italy

¹⁰ Università Politecnica delle Marche, via Breccie Bianche 12, 60131 Ancona, Italy

¹¹ Università degli Studi di Cassino e del Lazio Meridionale, DICeM, via Di Biasio 43, 03043 Cassino, Italy

¹² Department of Civil, Construction-Architecture and Environmental Engineering, University of Aquila, Via G. Gronchi 18, 67100 L'Aquila, Italy

Introduction

The seismic sequence recorded in central Italy in 2016–2017 included nine main events (Table 1) with moment magnitude (M_w) ≥ 5.0 (four of which were $M_w \geq 5.5$) occurring on four separate days (August 24th 2016, October 26th and 30th 2016 and January 18th 2017), as described in detail in Chiaraluce et al. (2017) and ISIDe Working Group (2016). The main events caused several observed changes in groundwater dynamics, including spring discharge variation, water-table anomalies and river discharge alteration in different basins located up to 100 km from the epicentral zone. The fractured and locally fissured carbonate nature of the aquifers outcropping in the earthquake area favors a quick co-seismic response in terms of pore pressure propagation; however, the observed sustained changes, which developed during several days after the main shocks, affected groundwater dynamics for several months after the seismic events.

Hydrogeological changes caused by earthquakes have been historically reported. Instrumentally measured responses, however, have become available only in the last few decades. These responses include changes in water level (Leggette and Taylor 1935; Cooper et al. 1965; Roeloffs 1998; Brodsky et al. 2003; Roeloffs et al. 2003; Lachassagne et al. 2011; Shi et al. 2015), temperature (Mogi et al. 1989), chemical composition (Claesson et al. 2004; Skelton et al. 2014), stream flow (Manga et al. 2003; Montgomery and Manga 2003; Manga and Rowland 2009; Muir-Wood and King 1993; Rojstaczer et al. 1995), and spring attributes (Wang and Manga 2015). Understanding the origin of these hydrological and hydrogeochemical phenomena may have significant impacts on the comprehension of the occurrence of liquefaction (Cox et al. 2012), water supply and quality (Gorokhovich and Fleegeer 2007), underground storage (Wang et al. 2013) and pore-pressure triggered seismicity (Brodsky et al. 2003).

The effects of earthquakes on groundwater are commonly divided into “transient oscillations” (Cooper et al. 1965) and

“sustained offset”, which include abrupt rises or falls and sustained gradual rise lasting for several days after the shock (Roeloffs 1998; Yan et al. 2014). The most frequent consequences of earthquakes are spring and river discharge increase and water-table rise, which are generally attributed to four general classes of possible explanations: (1) co-seismic static strain increases pore pressure that may contribute to change permeability (e.g. Wakita 1975; Jonsson et al. 2003); (2) earthquake-related dynamic strains may increase permeability, permitting a more rapid flow, which in fractured aquifers can be enhanced by fracture cleaning, eventually increasing discharge (e.g. Briggs 1991; Rojstaczer and Wolf 1992; Rojstaczer et al. 1995; Sato et al. 2000; Wang et al. 2004a; Curry et al. 1994; Amoruso et al. 2011); (3) breaching of hydraulic barriers or seals (e.g. Sibson 1994; Brodsky et al. 2003; Wang et al. 2004a); (4) the excess of water discharged after the earthquake lies in the shallowest subsurface where water is liberated by the consolidation or even liquefaction of near-surface unconsolidated materials (e.g. Manga 2001; Manga et al. 2003; Montgomery et al. 2003).

Looking at the relationships between tectonic framework, hydrogeological setting and earthquakes from a wider point of view, recent research activities have highlighted the role of fluids at crustal scale during the seismic cycle. Doglioni et al. (2014), for instance, suggest that fluid flow rates differ during the different periods of the seismic cycle (inter-seismic, pre-seismic, co-seismic and post-seismic periods), also in connection with the tectonic style. In particular, they hypothesize that in extensional tectonic settings like central Italy, the wedge of crust above the brittle ductile transition remains “suspended” while a dilated area forms during the inter-seismic period. This area would trap deep fluids, which when the wedge of crust above the brittle ductile transition starts to drop in the pre-seismic period, would be squeezed above due to the progressive fracture closing. Consequently, in the co-seismic period, aquifers can host changes in hydrochemistry (Barberio et al. 2017) and in water levels, independently from

Table 1 Seismic events with $M_w \geq 5.0$ recorded in central Italy between 24 August 2016 and 18 January 2017. Data from the four main events having $M_w \geq 5.5$ are highlighted in *italic*. Source: INGV (2017)

Date time (UTC)	M_w	Epicenter location	Depth (km)	Latitude	Longitude
August 24th 2016 01:36:32	<i>6.0</i>	Accumoli	<i>8.1</i>	<i>42.6983</i>	<i>13.2335</i>
August 24th 2016 02:33:28	5.3	Norcia	8.0	42.7922	13.1507
October 26th 2016 17:10:36	5.4	Castelsantangelo sul Nera	8.7	42.8802	13.1275
October 26th 2016 19:18:05	<i>5.9</i>	Castelsantangelo sul Nera	<i>7.5</i>	<i>42.9087</i>	<i>13.1288</i>
October 30th 2016 06:40:17	<i>6.5</i>	Norcia	<i>9.2</i>	<i>42.8322</i>	<i>13.1107</i>
January 18th 2017 09:25:40	5.1	Capitignano	10.0	42.5450	13.2768
January 18th 2017 10:14:09	<i>5.5</i>	Capitignano	<i>9.6</i>	<i>42.5310</i>	<i>13.2838</i>
January 18th 2017 10:25:23	5.4	Capitignano	9.4	42.5033	13.2770
January 18th 2017 13:33:36	5.0	Barete	9.5	42.4733	13.2747

changes due to the previously listed local mechanisms, which can affect the hydrodynamics of the struck aquifers during and after the seismic sequence. Such a comprehensive tectonic model allows looking at changes induced in groundwater after earthquakes in a general framework of crustal deformation, suggesting the role of deep inputs in triggering the aforementioned well-known processes (as pore pressure changes, permeability increase, liquefaction/consolidation, etc.) acting at the aquifer scale.

The effects of past earthquakes on groundwater in central Italy have been described by previous papers. Esposito et al. (2001) describe the effects of four earthquakes in southern Apennines including the 1980 Irpinia earthquake, which generated important hydrogeological changes as far as 200 km from the epicenter, including a significant increase of Caposele spring flow. Amoroso et al. (2011) describe the hydrogeological changes in a fractured aquifer after the L'Aquila 2009 earthquake, inferring that those changes were probably connected with the increase of bulk hydraulic conductivity at the aquifer scale, mainly due to fracture cleaning, raising hydraulic heads in the discharge zones, and correspondingly lowering them in the recharge areas (Adinolfi Falcone et al. 2012; Galassi et al. 2014).

The aim of this paper is to present an overview of the effects of the 2016–2017 seismic sequence on the dynamics of groundwater flow in central Apennines, analyzing the extent of the impacted area, possible relations between tectonic environments, geological-hydrogeological setting, and groundwater changes, and providing preliminary considerations on the possible causes of the observed phenomena.

Geological and hydrogeological framework

The central Apennines (Italy) is a Meso-Cenozoic ENE-dipping thrust-and-fold belt mainly developed during upper Miocene-Quaternary, composed by a pre-orogenic Triassic-Miocene sedimentary succession overlain by Miocene and Pliocene synorogenic sediments, resulting in a highly variable facies and thickness distribution. A Meso-Cenozoic carbonate platform domain extends in the SE part of the study area (Latium Abruzzi Apennine, Fig. 1), consisting of a 5,000-m-thick sequence of limestone and subordinate dolomite of Upper Triassic to upper Miocene age (Brandano and Loche 2014 and references therein). In the western side of the area (Umbro Marchean Apennine), a Lower Jurassic carbonate shelf unit is overlain by stratified pelagic sediments (middle Lias-lower Miocene), with an overall thickness of 2,500–3,000 m (Marchegiani et al. 1999). The Apennine orogenesis overthrusts the Umbria-Marche succession onto the Latium–Abruzzi platform along the main regional thrust

fault system named Olevano-Antrodoco line (Pierantoni et al. 2005 and references therein). From the upper Miocene to lower Pliocene, thrust migration towards the east was coupled with the progressive development of fore-deeps in front of the migrating fold-and-thrust belt (Cipollari and Cosentino 1995).

Since the upper Miocene–lower Pliocene, extensional faulting connected with the opening of the back-arc Tyrrhenian Basin has been dissecting the compressive structures (Boncio and Lavecchia 2000 and references therein), leading to the development of intermontane basins filled with thick continental sequences of Quaternary alluvial, detrital and lacustrine deposits (Cavinato and De Celles 1999). Some normal faults show evidence of Holocene activity, suggesting that they may be responsible for the seismic activity occurring in this sector of the Apennines (Cello et al. 1998), mainly confined within the upper part of the crust (<16 km; Lavecchia et al. 1994; Boschi et al. 1995).

In the study area, the 2016–2017 seismic sequence includes some of the largest instrumental earthquakes of the last 40 years (Norcia 1979 Mw = 5.9, Irpinia 1980 Mw = 6.9, Gubbio 1984 Mw = 5.2, Colfiorito 1997 Mw = 5.9, L'Aquila 2009 Mw = 6.3; Pantosti and Valensise 1990; Boncio and Lavecchia 2000; Deschamps et al. 2000; Chiarabba et al. 2009). The 2016–2017 sequence and its main shocks (Table 1) were generated by the Gorzano Mt.-Vettore Mt.-Bove Mt. faults (Galadini and Galli 2003, LMF and MVF in Fig. 2). The seismic crisis started with the August 24th 2016 event (Mw 6.0) and a further significant event on October 26th. The Vettore Mt. fault experienced a rupture with tectonic segments ~10 km long and a surface-displacement of ~30 cm (Smeraglia et al. 2017). The October 30th 2016 event (Mw 6.5) was generated by the rupture of the central zone of the fault by a normal movement. The focal mechanism, identical to the previous earthquakes, was a strike-angle of N155°, a WSW dip slip and a dip angle about of 50° in depth (RCMT 2016). During the October 30th 2016 event, the entire Vettore Mt.-Bove Mt. fault system gave origin to important surface faulting occurrences, reusing the pre-existing fault plane and displacing the fault segments previously broken.

The acquisition of the interferometric satellite data ALOS-2 from JAXA (Japan Aerospace Exploration Agency) and further interferometric analyses (INGV Central Italy Earthquake Team 2016) provided an estimation of the co-seismic subsidence along the NW–SE component reaching a maximum of ~80 cm (LOS: Satellite Observation Line). The horizontal co-seismic maximum movements consist of ~40 cm towards NE, ~30 cm towards SW as well as a maximum vertical movement of about 20–40 cm, when considering also the October 30th event (INGV Working Group GPS 2016; INGV Central Italy Earthquake Team 2016).

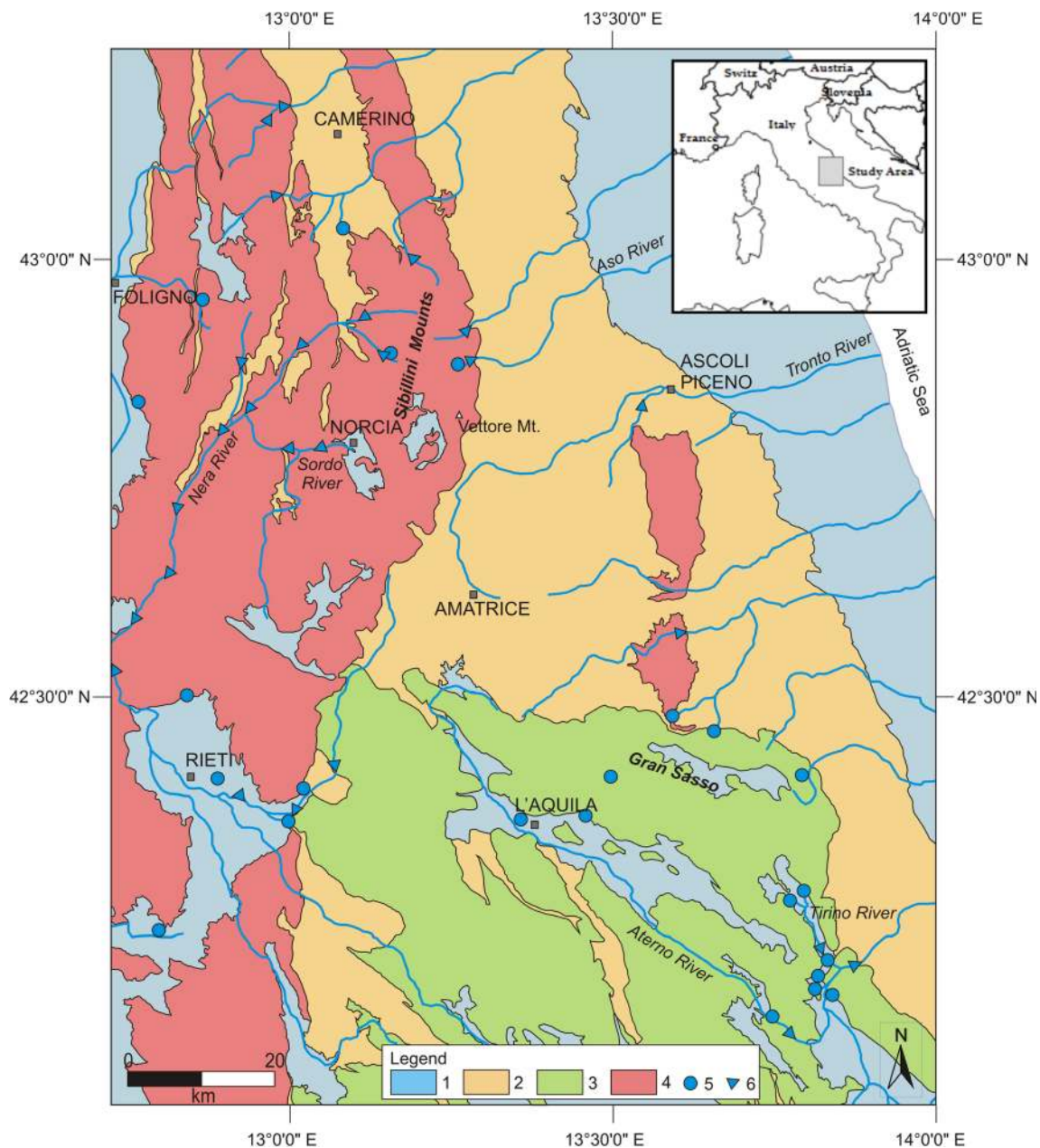


Fig. 1 Hydrogeological setting of the study area. 1 Alluvial aquifers and aquitards; 2 Synorogenic low-permeability deposits; 3 Latium-Abruzzi carbonate fractured aquifers; 4 Umbro-Marchean carbonate fractured

aquifers; 5 Main springs (mean discharge $>0.5 \text{ m}^3/\text{s}$); 6 Main streambed springs (mean discharge $>0.5 \text{ m}^3/\text{s}$)

In the study area, the fractured carbonate ridges host the main aquifers, feeding several perennial springs (Nanni and Vivalda 2005; Martarelli et al. 2008; Mastrorillo et al. 2009; Mastrorillo and Petitta 2014) with steady regimen, located mostly at the external boundaries of the aquifers (Fig. 1). Groundwater flows in fissured to locally karstified carbonates. The Miocene-Pliocene synorogenic silicoclastic sediments surrounding the carbonate aquifers, as well as the Plio-Quaternary deposits, filling the intermontane plains and the river valleys, act like aquitards (Petitta et al. 2011).

Widespread karst development, including endorheic basins, ensures high infiltration rates, from 500 to 700 mm/year, in the Umbria Marchean aquifers and up to 900 mm/year in the Latium-Abruzzi aquifers, collectively feeding a total discharge of about $300 \text{ m}^3/\text{s}$ (Boni et al. 1986, 2010). Fractures and karst conduits allow for fast vertical flow in the vadose zone, while the large thickness of the saturated zone facilitates a steady flow towards the basal springs that show outstandingly high and steady discharge (Petitta 2009; Amoroso et al. 2014; Fiorillo et al. 2015).

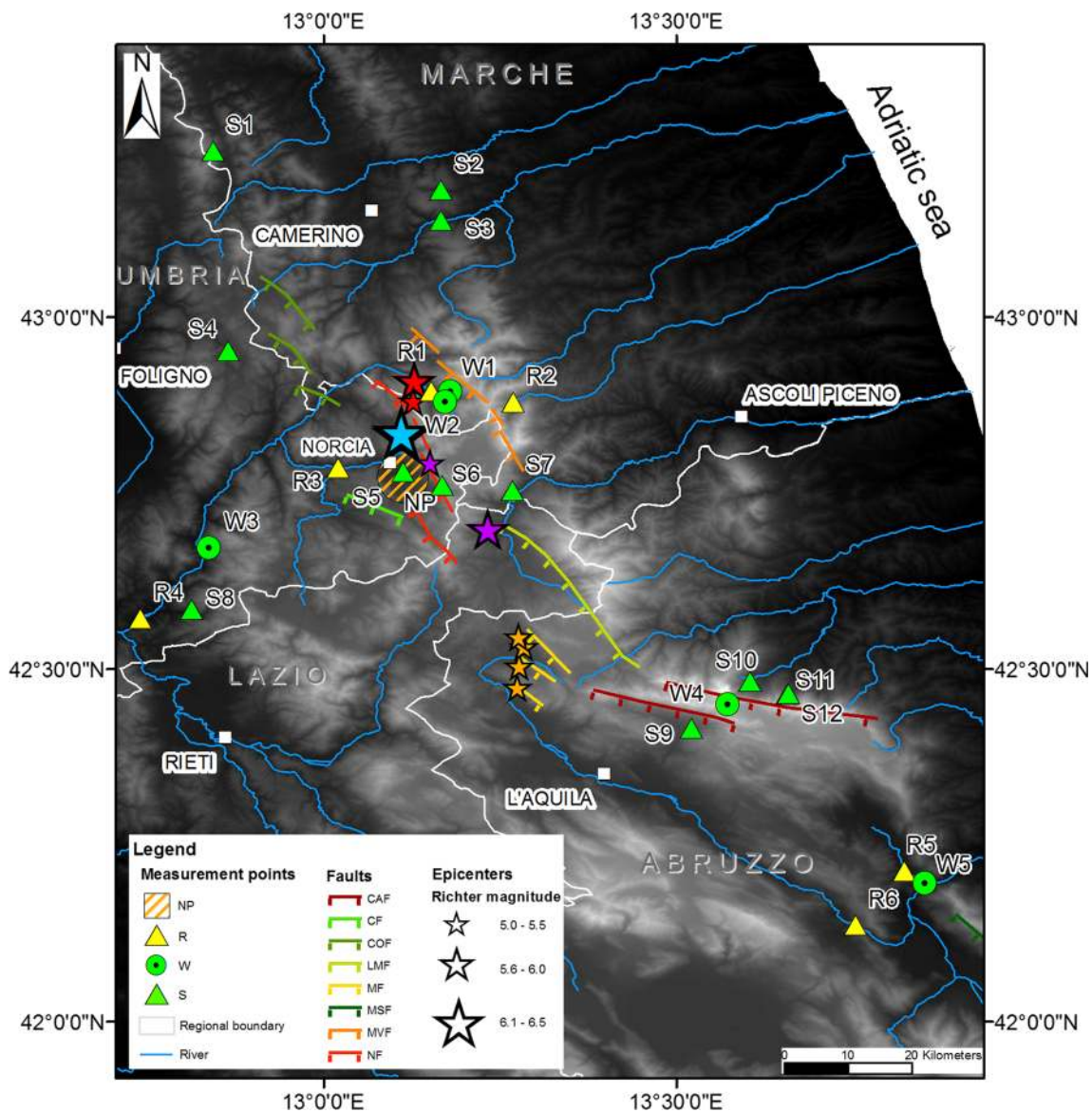


Fig. 2 Location of the measurement points, main epicenters and activated faults: R river gauge; W well; S spring. NP Norcia Plain. See Tables 2, 3 and 4 for details. Epicenters are represented by stars: August 24th 2016 event is in purple, October 26th 2016 in red, October 30th 2016 in cyan and January 18th 2017 in orange. Quaternary fault systems: MVF Monte

Vettore fault (Vettore-Bove faults); NF Norcia fault; CF Cascia fault; LMF Monti della Laga fault (Gorzano Mt.-Campotosto faults); MF Montereale fault; COF Colfiorito fault; CAF Campo Imperatore-Assergi fault; MSF Morrone-Sulmona fault. Source: INGV Central Italy Earthquake Team (2016)

Methodology

Co-seismic changes were examined in several observation sites located within the area affected by the earthquakes. Within the framework of a continuous monitoring, the collected data refer to piezometric heads in wells and piezometers, spring discharges and river hydrometric levels or discharges.

Collected data

Altogether, 22 automatic records from continuous monitoring sites were collected, plus one manually measured.

The monitoring site locations are shown in Fig. 2, distinguishing piezometric heads in monitoring wells (W1–W5), spring discharges (S1–S12) and hydrometric levels or discharge in river gauging stations (R1–R6). In addition, in February 2017, water-table levels in the porous local aquifer of the Norcia Plain (NP in Fig. 2) were recorded in 16 wells and compared to a piezometric map realized in 2011.

The monitored springs can be divided into the following: basal springs (S4, S5, S7 and S8), whose steady discharge shows limited seasonal variation; springs fed by shallow aquifers (S1, S2 and S3); and high-elevation springs (S6, S9, S10,

S11 and S12) having a seasonal slightly variable discharge. All the springs, except Torbidone (S5), are tapped for water supply systems.

The monitoring wells tap the basal aquifers at depths from 20 to 250 m. In some cases (W1, W2 and W3), the water level recordings were occasionally affected by the operations for the related water-supply systems. In detail, W1 and W2 were affected by operational changes in the tunnel drainage system of the near San Chiodo spring, whereas the disturbances prior to August 2016 in W3 were due to the works for the construction of a new aqueduct.

The discharge of the monitored rivers can be considered an indicator of hydrogeological changes at the basin scale, because a significant amount of groundwater directly feeds the rivers' baseflow by streambed springs. The rivers with catchment areas less than 100 km² (R1, R2, R3 and R5) have a steady regimen too and are predominantly fed by baseflow, whereas the runoff may be considered negligible. In the widest river basins (>1,000 km²; R4 and R6) the runoff contribution cannot be disregarded. It follows that the river discharge is more variable, despite the clear dominant role of baseflow.

Data have been recorded by regional hydrographic services, water supply companies or directly by the research teams monitoring the earthquake zones. All available data from June 1st 2016 to February 28th 2017 were considered. Public service data are available on-line (ARPA Umbria 2017; Regione Marche 2017; Regione Umbria 2017).

Methods of data measurement

Water-table depths have been recorded in wells and piezometers by downhole data loggers with atmospheric compensation. The horizontal piezometer W4, located in the underground National Institute for Nuclear Physics (INFN) laboratory, measures the hydraulic head (pressure in MPa) by a 3-channel 24-bit ADC (Analog to Digital Converter; De Luca et al. 2016). To quantify local head changes during each seismic event, only W4 original pressure data were converted (approximately) to water-table elevation by multiplying the pressure (MPa) by 100 and adding the obtained elevation to the elevation of the top of the borehole (987 m a.s.l.).

Spring discharges have been measured by automatic water level sensors in weirs or in Venturi tubes, and converted into discharge through the related rating curve. Only for the Torbidone spring, was the discharge manually measured with a portable flow meter, starting on November 11th 2016 at a frequency of one measurement about every 5 days. River gauging stations are equipped with water-height data loggers or automatic ultrasonic measurement sensors. Rating curves,

where available, have been used in conjunction with stage measurements to determine the river discharges.

Methods of data processing

Because of the different nature of data sources, the time series from continuous monitoring may have different measurement frequency, with intervals ranging from 0.05 s to 24 h. To ensure uniformity, data have been aggregated and analyzed at daily scale.

The mean discharge of each data series was calculated considering the time intervals before, between and after the four major seismic events of $M_w \geq 5.5$. The first interval corresponds to the period before the first main seismic event, and the second, the third and the fourth ones identify the time intervals between the first–second, second–third and third–fourth main events; the last one corresponds to the period after the fourth main event. The discharge/level variation associated with each one of the four main events was calculated as the difference between the daily value prior to and after each event. In cases where the changes were very abrupt and the difference between the daily values was not appreciable, hourly values were considered. Where even the hourly difference was not evident, changes have been considered as “not significant” (NS). All calculated values are shown in Tables 2, 3 and 4.

Results

Figures 3, 4, 5 and 6 show the time plots of the available data from monitoring sites (location in Fig. 2), summarized in Tables 2, 3 and 4, which refer respectively to water levels in piezometers (W1–W5), spring discharge (S1–S12) and river discharge or levels (R1–R6). Red bars in Figs. 3, 4, 5 and 6 indicate the four main $M_w > 5.5$ events. For the sake of simplicity, the August 24th 2016, October 26th 2016, October 30th 2016 and January 18th 2017 earthquakes will be named hereinafter 1st, 2nd, 3rd and 4th events respectively. See Fig. 2 for the locations of epicenters and the main active fault systems. Both the 1st and the 2nd events were clearly perceived in the S1, S2 and S3 northern sites (Fig. 3a), with abrupt step-like variations. The 3rd event, the strongest of the sequence, only slightly affects the discharge at S1 and S3.

Further south, Forca Canapine spring and Pescara spring (S6 and S7, Fig. 3b) show a clear increase of discharge after the 1st event, more step-like for S6 but gradual and sustained for S7. These two springs are located at high elevation (1,350 and 850 m a.s.l.) and they both suffered for a sharp decrease after the 3rd event, which completely dry up at S6. Aso River nearby (R2, Fig. 3b),

Table 2 Water table changes caused by the four main seismic events ($M_w \geq 5.5$)

Site ID	Name	Elevation (m a.s.l.)	Average level EQ1 (m a.s.l.)	Δ Water level EQ1 (m)	Average level post EQ1 (m a.s.l.)	Δ Water level EQ2 (m)	Average level post EQ2 (m a.s.l.)	Δ Water level EQ3 (m)	Average level post EQ3 (m a.s.l.)	Δ Water level EQ4 (m)	Average level post EQ4 (m a.s.l.)
W1	PIEZ. D	779	759.94	+2.17	761.91	+1.22	763.58	+6.96	770.05	0	769.21
W2	PIEZ. G	823	775.54	-1.07	777.02	-1.14	777.39	+6.05	781.23	0	780.57
W3	Renari di Capriglia	329	295.61	+0.62	296.95	NA	NA	NA	NA	NA	NA
W4	Borehole S13	987	1252	+1.00	1253	0	1196	+1.10	1198	+0.20	1194
W5	Bussi sul Tirino	238	226.27	+0.28	226.07	+0.04	225.96	+0.21	225.81	+0.82	226.14

EQ1: August 24th 2016 seismic event. *EQ2*: October 26th 2016 seismic event. *EQ3*: October 30th 2016 seismic event. *EQ4*: January 18th 2017 seismic event. Negative changes are highlighted in *italic*. NA not available value

Table 3 Spring discharge variations caused by the four main seismic events ($M_w \geq 5.5$)

Site ID	Name	Elevation (m a.s.l.)	Average discharge pre EQ1 (m^3/s)	Δ Discharge EQ1 (m^3/s)	Average discharge post EQ1 (m^3/s)	Δ Discharge EQ2 (m^3/s)	Average discharge post EQ2 (m^3/s)	Δ Discharge EQ3 (m^3/s)	Average discharge post EQ3 (m^3/s)	Δ Discharge EQ4 (m^3/s)	Average discharge post EQ4 (m^3/s)
S1	Montenero	840	0.057	+0.002	0.044	+0.015	0.050	NS	0.064	NS	0.062
S2	Nicolini	470	0.073	+0.010	0.061	+0.016	0.078	NS	0.060	NS	0.072
S3	Valcimarra	310	0.032	+0.004	0.020	+0.008	0.020	+0.005	0.020	NS	NA
S4	Alzabove	640	0.298	+0.019	0.278	+0.011	0.269	+0.008	0.259	0	0.256
S5	Torbidone	610	0	0	0	0	0	+1.510	0.990	NS	1.450
S6	Forca Camapine	1350	0.030	+0.045	0.021	+0.003	0.029	-0.029	0	NS	0
S7	Pescara	850	0.259	+0.129	0.350	-0.012	0.337	-0.059	0.242	NS	0.240
S8	Lupa	375	0.115	+0.0003	0.091	+0.0005	0.075	+0.004	0.072	NS	0.062
S9	Assergi	967	0.495	+0.058	0.515	NS	0.515	+0.045	0.515	+0.019	0.486
S10	Ruzzo	964	0.979	+0.016	0.995	NS	0.995	+0.085	0.922	NA	NA
S11	Vaccelliera bassa	937	0.193	+0.019	0.200	NS	0.200	+0.021	0.211	NA	NA
S12	Vaccelliera alta	1015	0.134	+0.021	0.140	NS	0.140	+0.019	0.146	NA	NA

EQ1: August 24th 2016 seismic event. *EQ2*: October 26th 2016 seismic event. *EQ3*: October 30th 2016 seismic event. *EQ4*: January 18th 2017 seismic event. Negative changes are highlighted in *italic*. NA not available value, NS not significant change

Table 4 River discharge and hydrometric river level variations caused by the four main seismic events ($M_w \geq 5.5$)

Site ID	Name	Elevation m a.s.l.	Average discharge pre EQ1 (m^3/s)	Δ Discharge EQ1 (m^3/s)	Average discharge post EQ1 (m^3/s)	Δ Discharge EQ2 (m^3/s)	Average discharge post EQ2 (m^3/s)	Δ Discharge EQ3 (m^3/s)	Average discharge post EQ3 (m^3/s)	Δ Discharge EQ4 (m^3/s)	Average discharge post EQ4 (m^3/s)
R1	Nera at Castelsantangelo	725	1.760	+0.360	2.060	+0.155	2.180	+2.340	4.260	NS	4.290
R2	Aso at Foce	950	0.574	+0.118	0.647	NS	0.682	NS	NA	NA	NA
R3	Sordo at Serravalle	510	2.448	+0.179	3.450	NA	3.890	+2.680	5.440	NS	6.901
R4	Nera at Torre Orsina	231	23.214	+1.533	23.459	+2.390	24.888	+5.160	30.738	NS	30.749
R5	Tirino at Madonna	313	0.85 ^a	NS	0.85 ^a	NS	0.85 ^a	NS	0.84 ^a	+0.14 ^a	0.84 ^a
R6	Aterno at Molina	454	0.23 ^a	NS	0.3 ^a	NS	0.35 ^a	NS	0.38 ^a	+0.17 ^a	0.40 ^a

^a Hydrometric river level (m)

EQ1: August 24th 2016 seismic event. EQ2: October 26th 2016 seismic event. EQ3: October 30th 2016 seismic event. EQ4: January 18th 2017 seismic event.

NA not available value, NS not significant change

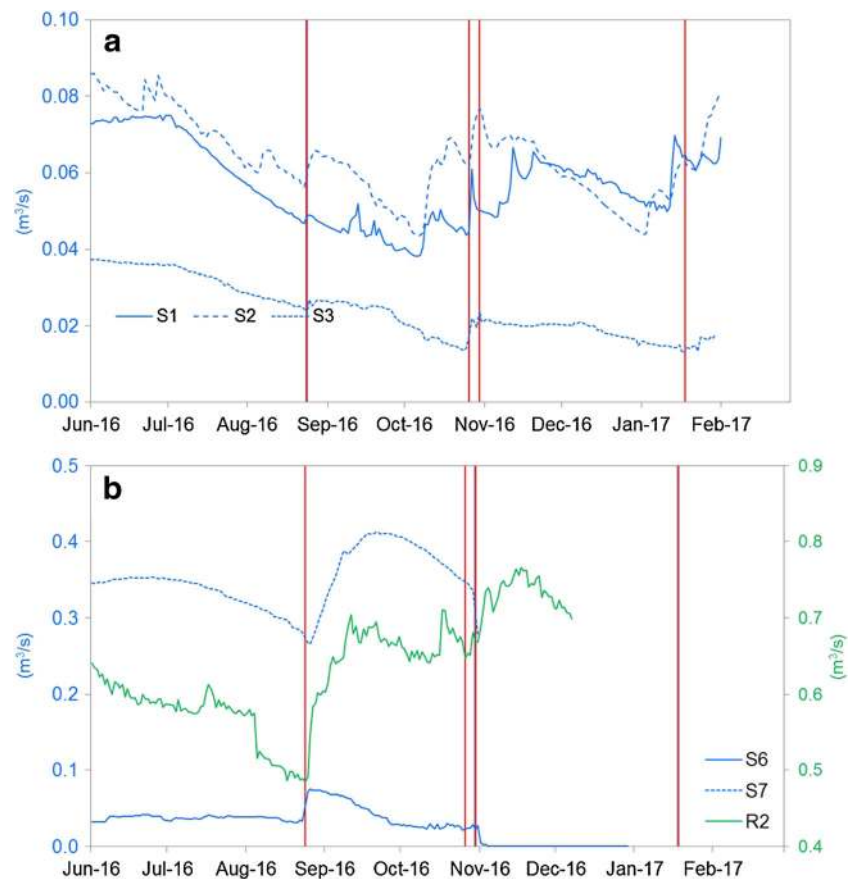
monitored at the spring outlet, is also clearly influenced by the 1st event with a step-like increase and limitedly affected by the following events.

Different effects were registered in the area closest to the 2nd and 3rd events, in the San Chiodo spring area (Fig. 4a) and in the Norcia area (Fig. 4b). In the San Chiodo area (Fig. 4a) a water supply system is operating by a tunnel drainage; periodical operational changes, opening and closing of different drainage tunnels, produce clear variations in the water levels (black vertical dashed lines in Fig. 4a). The responses of two of the 14 available piezometers (W1 and W2), considered representative of the entire monitoring network, and the discharge of the Upper Nera River downstream at Castelsantangelo (R1), are shown. After the 1st event, the system reacted with a sharp step-like increase in the downgradient part of the aquifer (W1, 779 m a.s.l.) and a clear step-like decrease in the upper part of the aquifer (W2, 823 m a.s.l.). The same happened on the 2nd event, while on the 3rd event the water level in W1 increased gradually by nearly 7 m, while in W2 it firstly decreased, then steadily increased for several days up to 6 m in height. After the 3rd event, the discharge of the Upper Nera River (R1) doubled; this quick increase reached a steady state in December 2016. In the Norcia area (Fig. 4b) the Torbidone spring (S5), reactivated after the 3rd shock, shows a gradual increase in discharge up to 1.5 m^3/s in about 3 months after the shock. The Sordo River (R3), receiving the Torbidone discharge, also reacted with a clear gradual and sustained increase lasting several months, due also to a different direct groundwater inflow. In addition, the water table of the porous clastic aquifer of the Norcia Plain has shown a hydraulic head increase, reaching +15 m at the contact with the carbonate aquifer, with respect to the water table recorded in 2010–2011.

The western-located S4, S8 and W3 (Fig. 4c) registered abrupt positive step-like increases for the 1st, 2nd and 3rd events, with some differences among them. The Nera River at Torre Orsina (Fig. 4d) receives the entire inflow of the aforementioned flow systems, and others not described here due to the absence of recordings; however, its discharge is clearly influenced by the 1st, 2nd and 3rd events, as shown by the abrupt step-like increases coincident with the first three red lines. Although no significant precipitation is recorded, the river discharge did not decrease for the 3 months following the 3rd event. Overall, the Nera River suffered for a total discharge increase of about 9 m^3/s considering the first three main events, corresponding to about 30% surplus of its natural baseflow.

The 4th event, which is the southernmost, was not perceived at all so far to the north, but locally affected the southern monitoring points (Fig. 5), located very close to its epicenter (Fig. 2). All four springs (Fig. 5a) show significant abrupt step-like increase of the discharge after the

Fig. 3 Daily discharge (m^3/s) of northern monitoring sites. **a** Central Marche; **b** Mt. Sibillini eastern slope. See Fig. 2 for location and Tables 3 and 4 for site characteristics. Vertical red bars locate the four main seismic events (Table 1)



1st and the 3rd event, while the 2nd event does not at all modify the hydrographs. The 4th event, in spite of being so close, only slightly influences the discharge of the sole S9 station.

Similar evidence has been recorded at a horizontal borehole (W4, Fig. 6) located in the underground laboratories of the INFN in the Gran Sasso massif (Petitta and Tallini 2002; Amoruso et al. 2013). The time plot of the pressure head variation shows sudden increases in the hydraulic pressure (MPa) with a sharp rise of about 2 m recorded on the 1st and on the 3rd events, while no evidence was recorded after the 2nd and 4th events (Fig. 6).

Further south, changes in the water table were clearly recorded in the monitoring well at Bussi sul Tirino (W5, Barberio et al. 2016; Fig. 5b). The magnitude of the water level variation is about 20 cm for the first three events, with a gradual sustained type variation, while an abrupt step-like increase up to 90 cm is observed for the closest 4th event. The river monitoring sites R5 and R6 do not show any significant variation of the hydrometric level in the 1st, 2nd and 3rd events (Fig. 5b). However, after the 4th earthquake, both the Aterno River (R6) and, most clearly, the Tirino River (R5) hydrometric level responses show a sharp and sudden increase of the hydrometric levels, which drop rather quickly to nearly the prior level than the earthquake discharge.

Discussion

The hydrogeological changes caused by the 2016–2017 seismic sequence are of remarkable intensity specially if compared to the relatively limited magnitude of the events; similar or larger hydrological responses are very rare (Mohr et al. 2015). The estimated amount of extra discharge drained by springs and rivers since August 24th 2016 for the following 6 months exceeds 0.1 km^3 . This amount has been obtained looking at the discharge of the entire Nera Basin (R4, Nera at Torre Orsina) before and after the seismic sequence: the additional discharge was about $1.5 \text{ m}^3/\text{s}$ between the 1st and 3rd event (about $8 \times 10^6 \text{ m}^3$), and about of $9 \text{ m}^3/\text{s}$ after the 3rd event, which until the end of February 2017 correspond to more than 0.095 km^3 . This estimation does not consider other changes observed in other basins, which released a minor amount of discharge.

Other documented examples of earthquake induced groundwater release include (ordered by decreasing earthquake magnitude): the Maule Mw 8.8 earthquake in Chile (1.1 km^3 , Mohr et al. 2016), the Chi-Chi Mw 7.5 earthquake in Taiwan (0.7 km^3 , Wang et al. 2004b), and the Hebgen Lake (Mw 7.3, 0.5 km^3), Borah Peak (Mw 6.9, 0.3 km^3 ; Muir-Wood and King 1993; USGS 2017), and Loma Prieta earthquakes in the USA (Mw 6.9, 0.01 km^3 ; Rojstaczer et al. 1995); however, these are earthquakes larger than the central Italy

Fig. 4 Daily discharge (left vertical axis) and daily water-table levels (right vertical axis) of monitoring sites of the Nera River Basin. **a** San Chiodo spring area. Vertical dashed black lines represent changes caused by the water supply system management; **b** Norcia Plain area. Blue dots represent the manual measurements of Torbidone spring (S5) discharge; **c** western area; **d** Nera River closing station. See Fig. 2 for location and Tables 2, 3 and 4 for site characteristics. Vertical red bars locate the four main seismic events (Table 1)

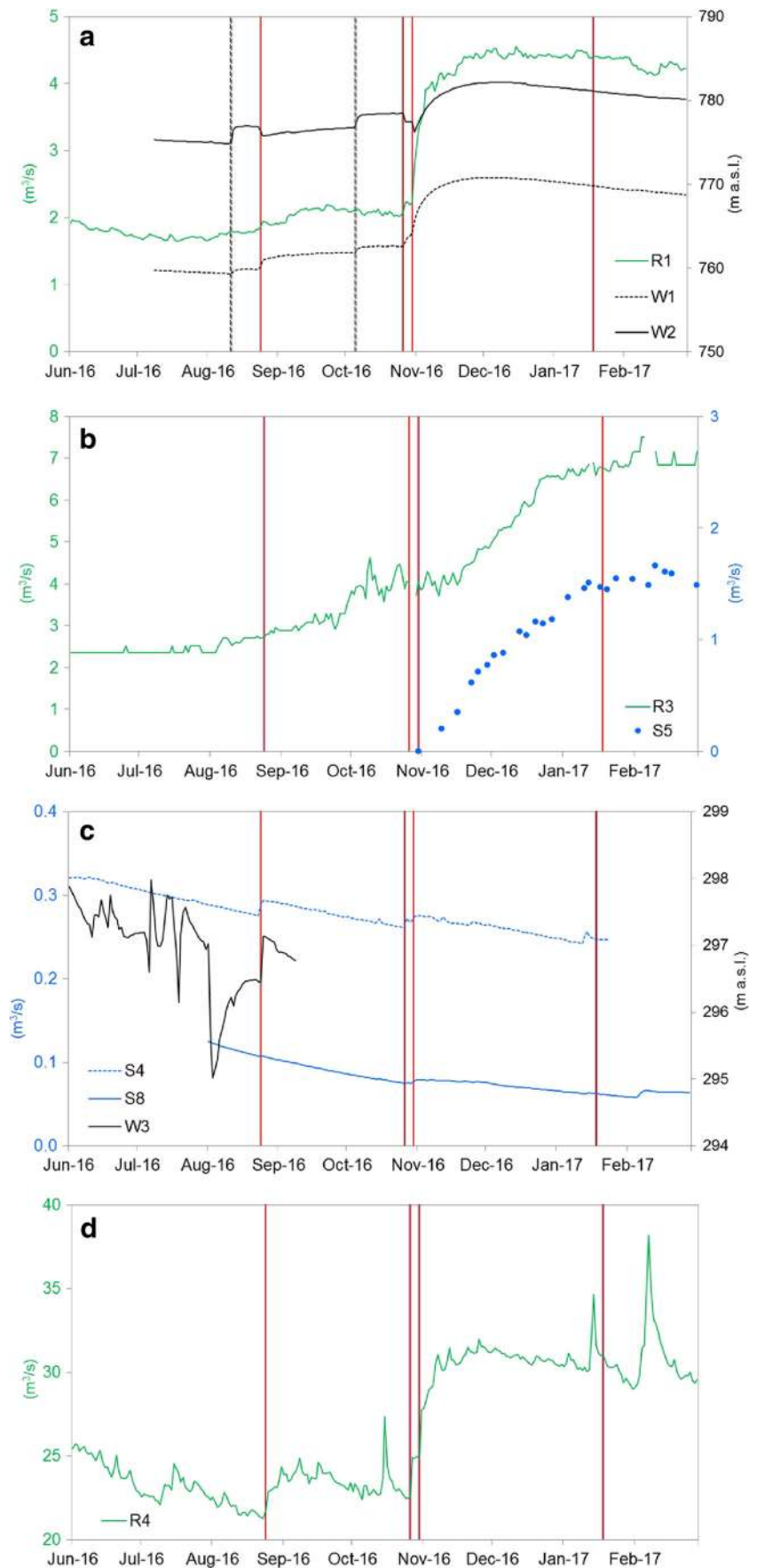
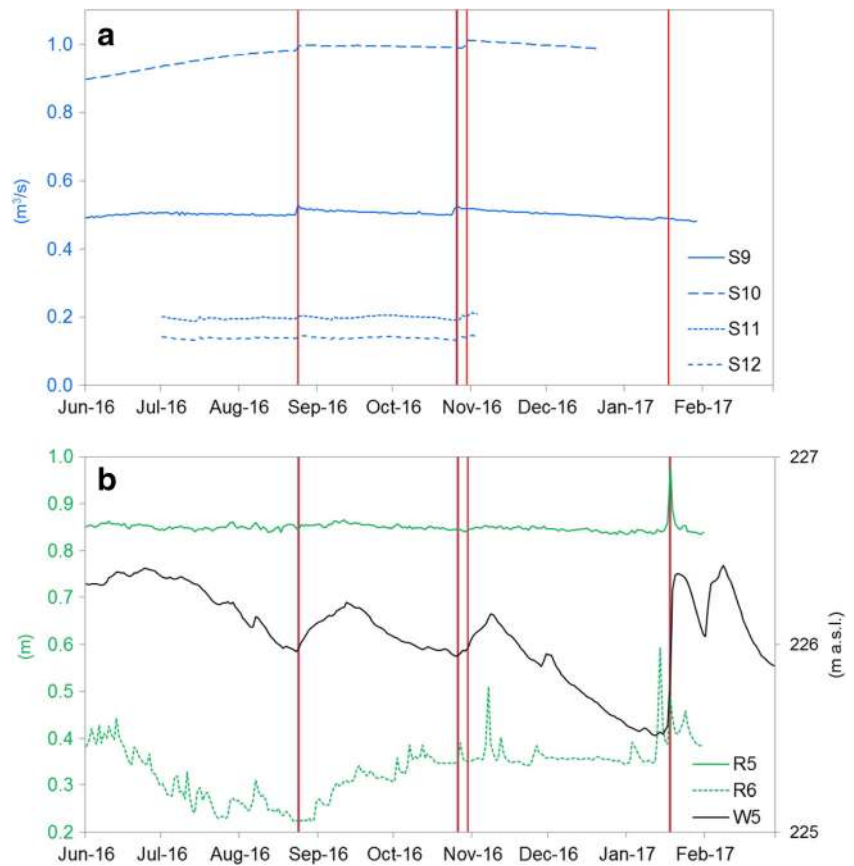


Fig. 5 Daily spring discharge, water level and hydrometric level of southern monitoring sites. **a** Gran Sasso springs; **b** Aterno–Tirino rivers (hydrometric levels on left vertical axis, water-table elevation on right vertical axis). See Fig. 2 for location and Tables 2, 3 and 4 for site characteristics. Vertical red bars locate the four main seismic events (Table 1)



events. At a comparable magnitude, the Mw 6.0 South Napa earthquake (USA) produced extra water of about 0.001 km³ (Wang and Manga 2015).

The extent of the area affected by hydrogeological changes approaches 10,000 km². The recorded hydrological variations fall in the known fields of abrupt and sustained water level changes in groundwater due to earthquakes (Fig. 7, modified from Wang and Chia

2008). Nevertheless, peculiar responses in the study area have been observed in sites very close to the epicenters (<10 km), where abrupt changes have been frequently followed by a sustained increase with time, especially after the 3rd event (October 30th), having the highest magnitude. This behaviour could be due to the fractured nature of the aquifer, where pressure changes can easily and quickly propagate along the effective porosity

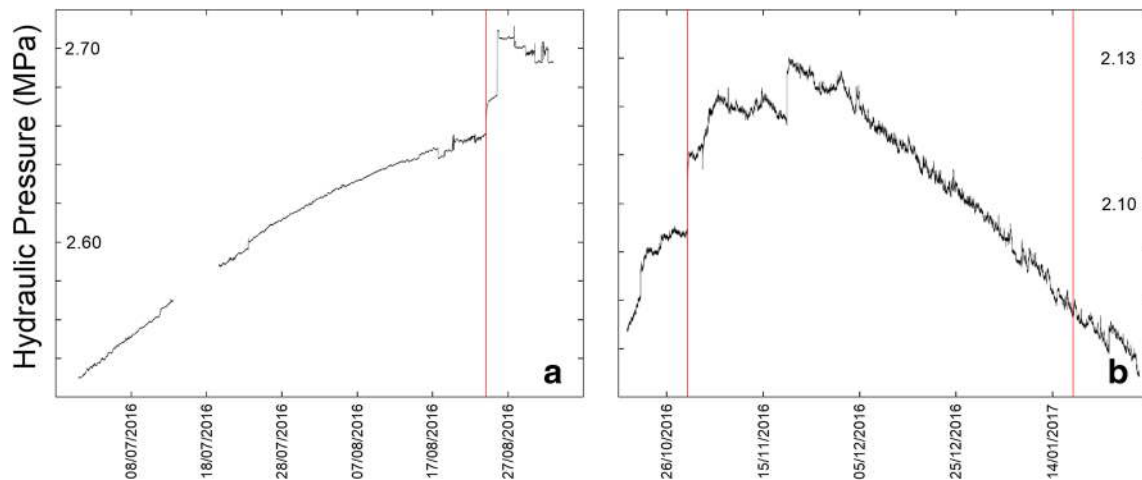


Fig. 6 Hydraulic pressure (MPa; Y-axis) vs. day (X-axis) of borehole W4. See Fig. 2 for location and Table 2 for site characteristics. The reported data are 1-min-averaged. Monitoring period **a** from July 1st

2016 to September 16th 2016 and **b** from October 22nd 2016 to January 31st 2017. The red lines refer to the August 24th, October 30th and January 18th earthquakes (Table 1)

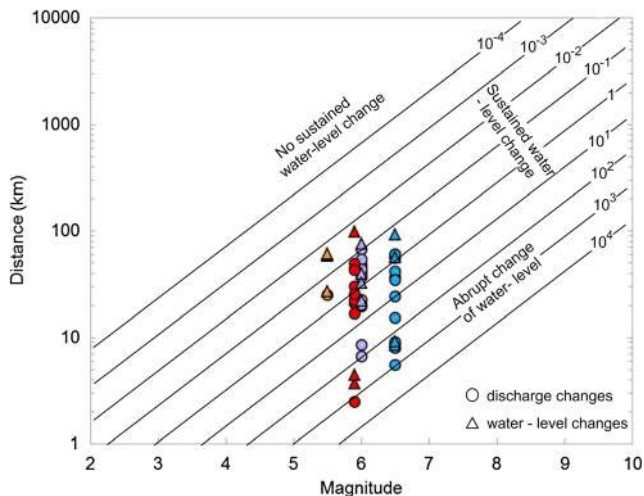


Fig. 7 Distribution of earthquake-triggered hydrogeological changes as a function of earthquake magnitude (horizontal axis) and epicentral distance (vertical axis). Also plotted are the contours (oblique lines) of constant seismic energy density (Wang and Manga 2010) and the domains where different types of coseismic water level responses occur (Wang and Chia 2008). The triangles represent the water level changes in wells or in rivers, the dots the discharge changes in spring or rivers. The four main events are distinguished by different colors: August 24th 2016 (Mw = 6) event is in purple, the October 26th 2016 (Mw = 5.9) event in red, the October 30th 2016 (Mw = 6.5) event in cyan and the January 18th 2017 (Mw = 5.5) event in orange

network, reaching the boundaries of the aquifers, causing change in hydrodynamic independently from seismic-induced stresses (Amoruso et al. 2011). Furthermore, the occurrence of several subsequent events repeatedly impacted the aquifers, as happened on October 30th 2016 for the third time in 2 months. Similar events have been not reported in the literature so far.

In addition, the characteristics of the fractured aquifers impacted by the shocks may also have influenced the

entity of the response. Differently from the Latium-Abruzzi carbonate aquifers, where a basal aquifer is usually governing groundwater flow, in the Umbria-Marchean aquifers, a network of interconnected faults plays a key role in determining the dynamic groundwater divide location, seepage velocity and extent of the recharge area. It follows that groundwater flow can be easily influenced by seismic events; furthermore, during the 2016–2017 sequence, the study area suffered from many earthquakes whose epicenters were differently located along the central Apennine chain; therefore, numerous aquifers and springs were hit by repeated events, or by a single group of seismic events only.

Generally, a decreasing intensity of the recorded effects was observed moving from the earthquake epicenters towards the distal areas. Figure 8 shows the spring discharge/water level variation, as a function of the distance between the monitored points and the epicenters of each seismic event. The result is a cloud of values from about 10–200% in the near-field (less than 10 km from epicenters), clearly decreasing with distance. Up to +50% in discharge and +2 m water level increase have been recorded between 20 and 30 km away, while minor changes have been observed for sites located between 60 and 100 km from the epicenters. Locally, discharge decreases have been encountered at less than 10-km distance from the epicentral area, but only for the October 30th event, which was the more energetic one.

The mechanism causing both sustained negative and positive hydraulic changes is frequently related to static stress modifications evidenced by comparison between pre-seismic and post-seismic conditions (Jonsson et al. 2003; Montgomery and Manga 2003; Parvin et al. 2014; Mohr et al. 2016). The difference between transient dynamic oscillations (Cooper et al. 1965) and the offset-type

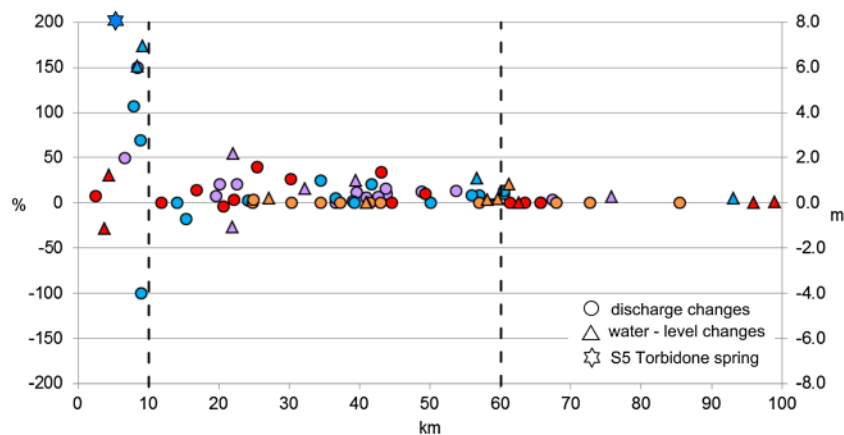
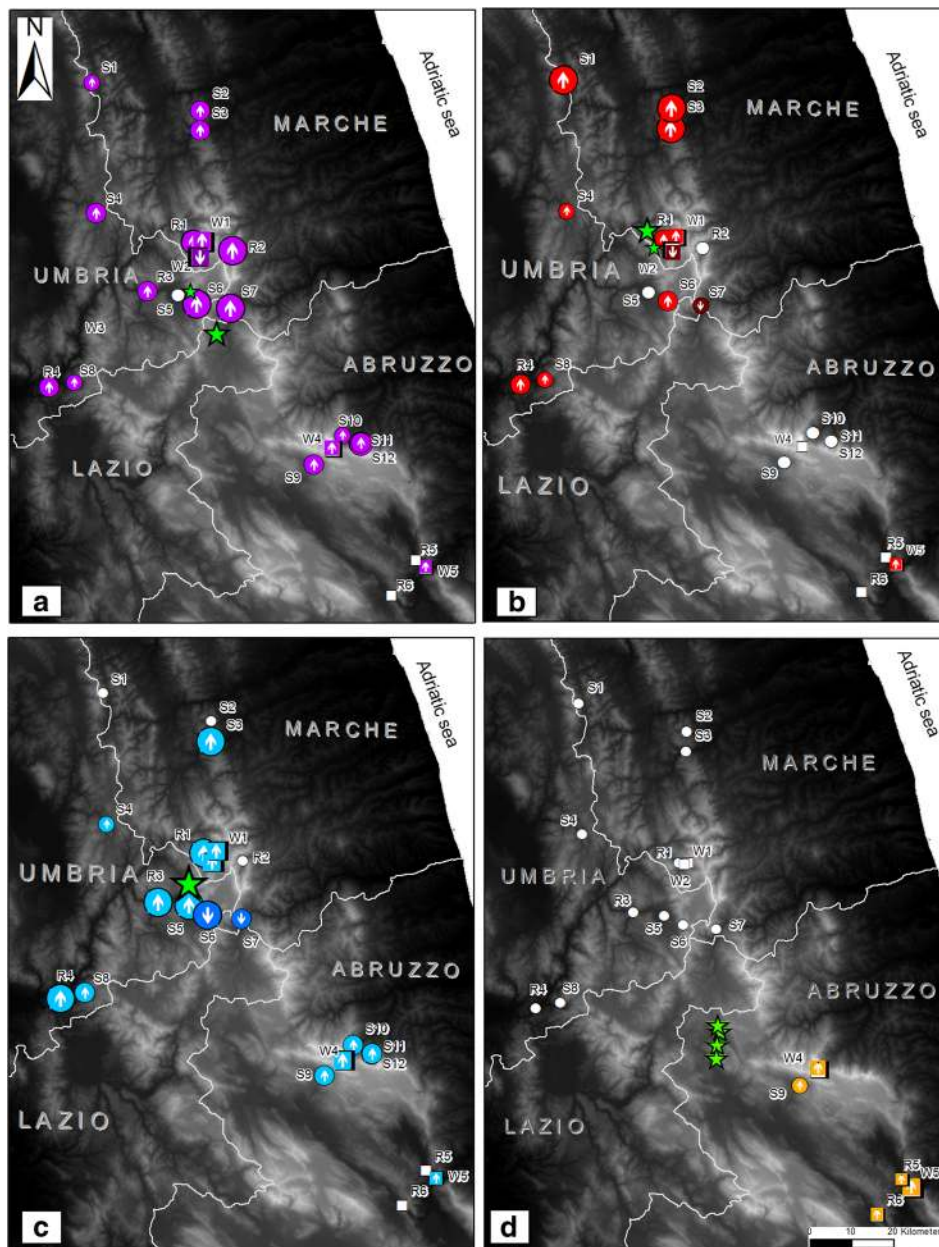


Fig. 8 Epicentral distance (horizontal axis) vs the discharge changes, expressed as a percentage of the pre-event period mean discharge (left vertical axis) and the water level changes (right vertical axis). Torbidone spring (S5), whose ratio to the pre-event discharge would be infinite (as the spring was dry prior to the earthquake) is marked by an asterisk at

200%. The four main events are represented by different colors: August 24th 2016 event is in purple, October 26th 2016 in red, October 30th 2016 in cyan and January 18th 2017 in orange. The vertical dashed lines show the changes in the near-affected area (<10 km from epicenters) and in a larger-affected area (up to 60 km from epicenters)



Legend

Discharge variation (%)	Water level variation (m)	Earthquake date	Epicenters
○ No variation	□ No variation	● August 24th 2016	★ Richter magnitude
● 0.01 - 5.00	■ 0.01 - 0.50	● October 26th 2016	★ 5.0 - 5.5
● 5.01 - 15.00	■ 0.51 - 1.00	● October 30th 2016	★ 5.6 - 6.0
● 15.01 - 20.00	■ > 1	● January 18th 2017	★ 6.1 - 6.5
● > 20			
⬆ Positive variation	⬆ Positive variation		
⬇ Negative variation	⬇ Negative variation		

Fig. 9 Maps of the entity and directional (positive or negative) changes in discharge (%) and in water level (m) after each main event: **a** August 24th 2016; **b** October 26th 2016; **c** October 30th 2016; **d** January 18th 2017

water-level changes affecting, in a more permanent way, groundwater flow, is also well described in Yan et al. (2014). Whereas the mechanism for explaining the first type of effects is substantially accepted as being transient oscillations due to crustal dynamic poro-elastic deformation in an aquifer during the passage of seismic waves (Rexin et al. 1962; Kitagawa et al. 2006; Yan et al. 2014), the cause of permanent offsets, corresponding to sustained changes, is still debated.

In this study case, the distribution of changes observed after each main event, and their positive or negative effects, are synthesized in Fig. 9. The impact on most of the springs is the increase of discharge with varying magnitude. Most of the recordings in wells and in rivers clearly indicated a sudden and sharp increase simultaneous with the earthquakes, generally followed by a steady increase lasting for a few days after the shock, and a subsequent smooth decrease. Few points show a decrease of water level or discharge: the disappearance of one tapped spring (S6) and a significant discharge decrease of the spring S7, both located at high elevation (Fig. 3b). Similar decreases or drying-up have been observed in other minor non-monitored springs located in the same recharge area. Another monitored site experiencing post-earthquake decrease in the water table is in Upper Nera Valley, where only the highest-elevation monitoring well (W2, Fig. 5a) suffered from a sharp lowering, quickly balanced in the following days.

The decrease of discharge or water levels and the disappearance of springs have been also been associated in literature to proximity to the active faults. With respect to the water-level changes observed in the footwall area of the fault activated by the Chi-Chi earthquake, Chia et al. (2001) report that water-level rise was the predominant effect in most of the area, whereas water-level fall prevailed in a narrow zone adjacent to the fault trace. Amoruso et al. (2011) report that after the L'Aquila Mw 6.3 earthquake, the two highest springs, located on the trace of the activated fault, suddenly dried up after the main shock. The opposite phenomenon, the reactivation of dry springs or stream, as observed in this case for the Torbidone spring (S5), is also well known. After the 2014 Mw 6.0 South Napa earthquake, many streams and springs, which were dry or nearly dry, started to flow after the earthquake (Wang and Manga 2015). The possible explanation given by the mentioned authors is the enhanced permeability in the recharge areas.

Generally, after the co-seismic peak, discharge and water levels remained on higher values with respect to pre-seismic conditions. A similar mechanism was observed after the 1980 Irpinia earthquake at Caposele spring (Esposito et al. 2001) and, more recently, in the Abruzzi region after the L'Aquila 2009 earthquake (Adinolfi Falcone et al. 2012). This last case has been explained by a double effect: (1) pore pressure

propagation due to dynamic stresses caused by the seismic waves, which determined the sudden peak, and (2) an increase of bulk hydraulic conductivity of the fractured aquifer due to fracture cleaning triggered by the pore pressure propagation, which induces mobilization by shaking fine particles that block fracture throats (Amoruso et al. 2011).

Recorded hydrological changes for the 2016–2017 earthquakes may be preliminarily attributed to the pore pressure propagation in the aquifers, which would be followed by a sustained discharge increase attributable to fracture cleaning, mobilizing fine particles from fractures (Brodsky et al. 2003; Wang and Manga 2010; Adinolfi Falcone et al. 2012), as reflected by turbidity increase, clearly recorded in several monitoring points (e.g. R1, S5, S11, S12). In this case, the superimposition of the post-seismic changes on a recession phase makes the post-earthquake evolution clearer. The dynamic stress due to pore pressure propagation has been clearly observed at the high-frequency-monitoring site W4 (Fig. 10), where the short-term (30 s) changes in hydraulic head are the response to the seismic wave of August 24th, whose effects on groundwater levels ended after a few minutes.

In this study, the sustained response of several monitored sites to the subsequent seismic events, considering the fractured nature of the struck aquifers, support the hypothesis of fracture cleaning and the consequent increase of the bulk hydraulic conductivity. In many cases, discharge increase has reached its peak a few days after one of the main events, followed by a decreasing trend due to the recession phase. Accordingly, in several cases, mainly located far from epicenters, the next earthquakes did not cause permanent changes, but only a temporary discharge increase, favoring the model of fracture cleaning. The location of negative effects at high-elevation sites confirms this hypothesis, as water-table decrease is expected in recharge zones of struck aquifers, while increase in discharge is common in low-elevation zones.

A more complex response has been recorded in the core area, i.e. between the epicenters of August 24th and October 30th events. In the Upper Nera River Valley (R1, W1 and W2), in the Norcia Plain (S5, R3) and partially in the eastern side of the Sibillini Mts. (S7, R2), the effects of both events is

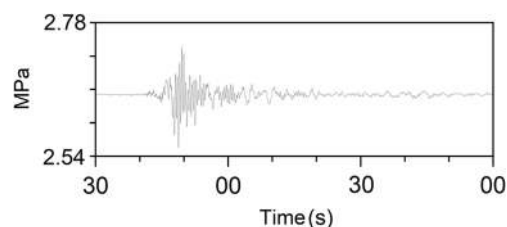


Fig. 10 Water pressure signal (in MPa) at W4 replicating the arrival of seismic waves of the August 24th event (modified from De Luca et al. 2016)

still evident in the following months. The discharge of springs and water-table elevations remained very high with respect to pre-earthquake conditions, as testified by the Nera main gauging station (R4), not simply justifiable by seismic stresses. The new conditions of groundwater flow are testified by the observed changes in the recession curve of San Chiodo spring (R1, W1, Fig. 5a): previous values of $\alpha = 0.003$ calculated for the 2011–2015 period, strongly decrease to $\alpha = 0.001$ after the earthquakes, testifying to a continuous additional contribution from the aquifer with time.

Consequently, other possible additional factors may have influenced the post-seismic response of the area of Sibillini Mts. The impressive increase of spring and river discharge observed in the Upper Nera River valley and Norcia plain in the mid-term responses, may be correlated with the subsidence induced by the toe of Vettore Mt. faulting, which might have created in the core of the Sibillini Mts. aquifer an additional “squeezing effect”. Other possible mechanisms, not further investigated in this paper, could be related to shaking of the aquifer, tilting, settlement and uplifting of the seismogenetic fault-bounded structures and the consequent dislocation of permeability thresholds induced by faulting. Further, a possible decrease in aquifer storativity due to fracture-width reduction could be envisaged, which would have directly triggered the additional volume of groundwater released in the months following the shocks, modifying groundwater dynamic divides and groundwater flow directions. This hypothesis, still not verified, should be carefully evaluated in the future, for prevision purposes.

The response of the monitored fractured aquifers to the earthquakes poses questions in terms of future management of groundwater resources of central Apennines. Furthermore, the discharge increase recorded along the Nera River basin has raised flood risks for the urban areas struck by the earthquake, as in Castelsantangelo sul Nera and Norcia. As several of the monitored springs are tapped for drinking purposes, it is necessary to carefully evaluate the consequences and the mid-to-long-term evolution of the spring discharge.

Conclusions

The abrupt and sustained variations of spring discharge and groundwater levels, observed in carbonate fractured aquifers in central Italy by a wide selection of water points during the 2016–2017 central Apennine seismic sequence, cannot be attributed to natural hydrological drivers and have therefore to be related to the earthquakes. The main findings obtained by analyzing data from more than 20 monitoring sites are the following:

1. The main shocks affected groundwater as far as 100 km from the epicenters, with instrumentally perceivable, sometimes dramatic, effects. A generalized decrease of the magnitude of the effects with distance was observed. The observed effects may be summarized as follows: (1) increase (rarely decrease) of heads measured in wells/piezometers, (2) positive (rarely negative) variations of spring discharge, (3) positive variation of river baseflow, (4) activation of historically intermittent springs, and (5) drying up of high-elevation springs. A quick oscillation, correlated with dynamic stresses, was observed in a few sites equipped with high-frequency recordings.
2. Within 6 months from August 24th 2016, more than 0.1 km³ of groundwater has been additionally discharged in the area (about +25% of the natural discharge). Comparison with similar case studies highlights the relatively high amount of discharge increase with respect to the limited magnitude of the seismic events; this peculiarity could be explained by the succession of four main events having $M_w > 5.5$, which continuously struck the fractured aquifers.
3. The observed response at regional scale is compatible with the cleaning of fractures and an overall mid-term increase of the bulk permeability due to the co-seismic pore-pressure propagation.
4. Eventually, the dramatic rise of the water table and of discharge in the core area could be the result of a “squeezing effect” due to the co-seismic subsidence in the Sibillini Mts. area, which would act on the storativity of the aquifer. A change in groundwater flow directions due to the tilting of the structure and the consequent dislocation of the permeability threshold induced by faulting could be an additional factor.

Based on the suggested conceptual models, two different evolutions of the groundwater flow could possibly be faced in the near future:

- If and where the fracture cleaning effect is solely responsible for discharge increase, gradually the spring and river discharge will return to previous values, without any permanent long-term effects; in this case, the additional volumes released by the aquifers will not be recovered, but in some years the groundwater system will probably regain its stability, as happened for the Gran Sasso aquifer after the 2009 earthquake;
- Alternatively, if and where the effective porosity and consequently the storativity of the aquifers (at least of the Sibillini Mts. area) have definitely decreased due to subsidence effects and/or fracture-width reduction, a share of the permanent reserves could be lost, and more perceivable effects would affect the groundwater system. In this case, long-term changes are expected in the regime of the springs, which would become

more impulsive, leading to a higher seasonal variation. Nevertheless, changes in the total amount of recharge, and consequently of discharge, are not expected, because possible storativity reduction does not influence the infiltration from rainfall.

Acknowledgements The authors are thankful to the following water supply companies and public bodies for making freely available spring or river discharge and water level data: Gran Sasso Acqua and Ruzzo Reti Companies; Nera aqueduct company (S.A.N. spa); CIIP S.P.A. Ascoli Piceno; A.S.SEM. S.p.A. San Severino Marche (MC); Azienda Specializzata Settore Multiservizi S.p.A. Tolentino (MC); APM Macerata; Multiservizi S.p.a. Ancona; Centro Funzionale Multirischi Protezione Civile Regione Marche; ARPA Umbria; Risorse Idriche e Rischio Idraulico Office of Regione Umbria; Ufficio Idrografico e Mareografico of Regione Abruzzo. Alessandro Lacchini, Luca Macerola and Mirco Marcellini are also acknowledged for data and map handling. Further, we wish to thank the reviewers for their useful comments and valuable remarks, which significantly improved our manuscript.

Open Access This article is distributed under the terms of the Creative Commons Attribution 4.0 International License (<http://creativecommons.org/licenses/by/4.0/>), which permits unrestricted use, distribution, and reproduction in any medium, provided you give appropriate credit to the original author(s) and the source, provide a link to the Creative Commons license, and indicate if changes were made.

References

- Adinolfi Falcone R, Carucci V, Falgiani A, Manetta M, Parisse B, Petitta M, Rusi S, Spizzico M, Tallini M (2012) Changes on groundwater flow and hydrochemistry of the Gran Sasso carbonate aquifer after 2009 L'Aquila earthquake. *Ital J Geosci* 131(3):459–474. <https://doi.org/10.3301/IJG.2012.05>
- Amoruso A, Crescentini L, Petitta M, Rusi S, Tallini M (2011) Impact of the April 6, 2009 L'Aquila earthquake on groundwater flow in the Gran Sasso carbonate aquifer central Italy. *Hydrol Process* 25(11):1754–1764. <https://doi.org/10.1002/hyp.7933>
- Amoruso A, Crescentini L, Petitta M, Tallini M (2013) Parsimonious recharge/discharge modeling in carbonate fractured aquifers: the groundwater flow in the Gran Sasso aquifer (central Italy). *J Hydrol* 476:136–146. <https://doi.org/10.1016/j.jhydrol.2012.10.026>
- Amoruso A, Crescentini L, Martino S, Petitta M, Tallini M (2014) Correlation between groundwater flow and deformation in the fractured carbonate Gran Sasso aquifer (INFN underground laboratories central Italy). *Water Resour Res* 50(6):4858–4876. <https://doi.org/10.1002/2013WR014491>
- ARPA Umbria (2017) Portata delle sorgenti [Discharge of the springs]. <http://www.arpa.umbria.it/articoli/portata-delle-sorgenti-000>. Accessed 3 Dec 2017
- Barberio MD, Billi A, Doglioni C, Lacchini A, Marinelli V, Petitta M (2016) Hydrogeological monitoring to assess possible pre-seismic correlations of groundwater changes with seismic activity in central Italy. *Rend Online Soc Geol It* 41:338–341. <https://doi.org/10.3301/ROL.2016.162>
- Barberio MD, Barbieri M, Billi A, Doglioni C, Petitta M (2017) Hydrogeochemical change before and during the 2016 Amatrice-Norcia seismic sequence. *Sci Rep* 7:11735. <https://doi.org/10.1038/s41598-017-11990-8>
- Boncio P, Lavecchia G (2000) A structural model for active extension in central Italy. *J Geodyn* 29(3–5):233–244. [https://doi.org/10.1016/S0264-3707\(99\)00050-2](https://doi.org/10.1016/S0264-3707(99)00050-2)
- Boni C, Bono P, Capelli G (1986) Schema idrogeologico dell'Italia Centrale [Hydrogeological scheme of central Italy]. *Mem Soc Geol It* 35:991–1012
- Boni C, Baldoni T, Banzato F, Cascone D, Petitta M (2010) Hydrogeological study for identification, characterization and management of groundwater resources in the Sibillini Mountains National Park (central Italy). *Ital J Eng Geol Environ* 2:21–39. <https://doi.org/10.4408/IJEGE.2010-02.O-02>
- Boschi E, Ferrari G, Gasperini P, Guidoboni E, Smriglio G, Valensise G (1995) Catalogo dei forti terremoti in Italia dal 461 a.C. Al 1980 [Catalog of earthquakes in Italy between 461 B.C. and 1980 A.C.]. Istituto Nazionale di Geofisica ING-SGA, Bologna
- Brandano M, Loche M (2014) The Coniacian-Campanian Latium-Abruzzi carbonate platform, an example of a facies mosaic. *Facies* 60(2):489–500. <https://doi.org/10.1007/s10347-013-0393-x>
- Briggs RO (1991) Effects of Loma Prieta earthquake on surface water in Waddell Valley. *JAWRA J Am Water Resour Assoc* 27(6):991–999. <https://doi.org/10.1111/j.1752-1688.1991.tb03148.x>
- Brodsky EE, Roeloffs EA, Woodcock D, Gall I, Manga M (2003) A mechanism for sustained ground water pressure changes induced by distant earthquakes. *J Geophys Res* 108(8):ESE7/1–ESE7/10. <https://doi.org/10.1029/2002JB002321>
- Cavinato GP, De Celles PG (1999) Extensional basins in the tectonically bimodal central Apennines fold-thrust belt, Italy: response to corner flow above a subducting slab in retrograde motion. *Geology* 27:956–959
- Cello G, Mazzoli S, Tondi E (1998) The crustal fault structure responsible for the 1703 earthquake sequence of central Italy. *J Geodyn* 26(2–4):443–460
- Chia YP, Wang YS, Wu HP, Chiu JJ, Liu CW (2001) Changes of groundwater level due to the 1999 Chi-Chi earthquake in the Choshui River fan in Taiwan. *Bull Seismol Soc Am* 91:1062–1068. <https://doi.org/10.1785/0120000726>
- Chiarabba C, Amato A, Anselmi M, Baccheschi P, Bianchi I, Cattaneo M, Cecere G, Chiaraluce L, Ciaccio MG, De Gori P, De Luca G, Di Bona M, Di Stefano R, Faenza L, Govoni A, Improta L, Lucente FP, Marchetti A, Margheriti L, Mele F, Michelini A, Monachesi G, Moretti M, Pastori M, Piana Agostinetti N, Piccinini D, Roselli P, Seccia D, Valoroso L (2009) The 2009 L'Aquila (central Italy) Mw6.3 earthquake: main shock and aftershocks. *Geophys Res Lett* 36:L18308. <https://doi.org/10.1029/2009GL039627>
- Chiaraluce L, Di Stefano R, Tinti E, Scognamiglio L, Michele M, Casarotti E, Cattaneo M, De Gori P, Chiarabba C, Monachesi G, Lombardi A, Valoroso L, Latorre D, Marzorati S (2017) The 2016 central Italy seismic sequence: a first look at the mainshocks, aftershocks, and source models. *Seismol Res Lett* 88(3):757–771. <https://doi.org/10.1785/0220160221>
- Cipollari P, Cosentino D (1995) Miocene unconformities in the central Apennines: geodynamic significance and sedimentary basin evolution. *Tectonophysics* 252:375–389
- Claesson L, Skelton A, Graham C, Dietl C, Mörth M, Torssander P, Kockum I (2004) Hydrogeochemical changes before and after a major earthquake. *Geology* 32:641–644. <https://doi.org/10.1130/G20542.1>
- Cooper HH, Bredehoeft JD, Papadopoulos IS, Bennett RR (1965) The response of well-aquifer systems to seismic waves. *J Geophys Res* 70:3915–3926
- Cox SC, Rutterb HK, Sims A, Manga M, Weir JJ, Ezzy T, White PA, Horton TW, Scott D (2012) Hydrological effects of the MW 7.1 Darfield (Canterbury) earthquake, 4 September 2010, New Zealand. *N Z J Geol Geophys* 55(3):231–247. <https://doi.org/10.1080/00288306.2012.680474>

- Curry RR, Emery BA, Kidwell TG (1994) Sources and magnitudes of increased streamflow in the Santa Cruz Mountains for the 1990 water year after the earthquake. In: Rojstaczer S (ed), The Loma Prieta, California, Earthquake of October 17, 1989-Hydrologic Disturbances, Geol Surv Prof Pap 1551-E, pp 31–50
- De Luca G, Di Carlo G, Tallini M (2016) Hydraulic pressure variations of groundwater in the Gran Sasso underground laboratory during the Amatrice earthquake of August 24, 2016. *Ann Geophys* 59, Fast Track 5. <https://doi.org/10.4401/AG-7200>
- Deschamps A, Courboulex F, Gaffet S, Lomax A, Virieux J, Amato A, Azzara A, Castello B, Chiarabba C, Cimini GB, Cocco M, Di Bona M, Margheriti L, Mele F, Selvaggi G, Chiaraluce L, Piccinini D, Ripepe M (2000) Spatio-temporal distribution of seismic activity during the Umbria-Marche crisis 1997. *J Seismol* 4(4):377–386. <https://doi.org/10.1023/A:1026568419411>
- Dogliani C, Barba S, Carminati E, Riguzzi F (2014) Fault on-off versus coseismic fluids reaction. *Geosci Front* 5(6):767–780. <https://doi.org/10.1016/j.gsf.2013.08.004>
- Esposito E, Pece R, Porfido S, Tranfaglia G (2001) Hydrological anomalies connected to earthquakes in southern Apennines (Italy). *Nat Hazards Earth Syst Sci* 1(3):137–144. <https://doi.org/10.5194/nhess-1-137-2001>
- Fiorillo F, Petitta M, Preziosi E, Rusi S, Esposito L, Tallini M (2015) Long-term trend and fluctuations of karst spring discharge in a Mediterranean area (central-southern Italy). *Environ Earth Sci* 74(1):153–172. <https://doi.org/10.1007/s12665-014-3946-6>
- Galadini F, Galli P (2003) Paleoseismology of silent faults in the central Apennines (Italy): the Mt. Vettore and Laga Mts. faults. *Ann Geophys-Ital* 46(5):815–836
- Galassi DM, Lombardo P, Fiasca B, Di Cioccio A, Di Lorenzo T, Petitta M, Di Carlo P (2014) Earthquakes trigger the loss of groundwater biodiversity. *Sci Rep* 4:6273. <https://doi.org/10.1038/srep06273>
- Gorokhovich Y, Fleeger G (2007) Pymatuning earthquake in Pennsylvania and late Minoan crisis on Crete. *Water Sci Technol Water Supply* 7(1):245–251. <https://doi.org/10.2166/ws.2007.028>
- INGV (2017) INGV Centro Nazionale Terremoti [INGV National Center for Earthquakes]. <http://cnt.rm.ingv.it>. Accessed 3 Dec 2017
- INGV Central Italy Earthquake Team (2016) Summary report on the October, 30 2016 earthquake in central Italy Mw 6.5. <https://doi.org/10.5281/zenodo.166238>
- INGV Working Group GPS (GPS data and data analysis center) (2016) Preliminary co-seismic displacements for the October 26 (Mw5.9) and October 30 (Mw6.5) central Italy earthquakes from the analysis of GPS stations Zenodo. <https://doi.org/10.5281/zenodo.167959>
- ISIDe Working Group (2016) Italian seismological and parametric database, version 1.0. <https://doi.org/10.13127/ISIDe>
- Jonsson S, Segall P, Pedersen R, Bjornsson G (2003) Post earthquake ground movements correlated to pore-pressure transients. *Nature* 424(6945):179–183. <https://doi.org/10.1038/nature01776>
- Kitagawa Y, Koizumi N, Takahashi M, Matsumoto N, Sato T (2006) Changes in groundwater levels or pressures associated with the 2004 earthquake off the west coast of northern Sumatra (M9.0). *Earth Planets Space* 58(2):173–179
- Lachassagne P, Leonardi V, Vittecoq B, Henriot A (2011) Interpretation of the piezometric fluctuations and precursors associated with the November 29, 2007, magnitude 7.4 earthquake in Martinique (lesser Antilles). *C R Geosci* 343:760–776. <https://doi.org/10.2016/j.crte.2011.09.002>
- Lavecchia G, Brozzetti F, Barchi M, Menichetti M, Keller JVA (1994) Seismotectonic zoning in east-central Italy deduced from an analysis of the Neogene to present deformations and related stress fields. *Geol Soc Am Bull* 106(9):1107–1120
- Leggette RM, Taylor GH (1935) Earthquakes instrumentally recorded in artesian wells. *Bull Seism Soc Am* 25:169–175
- Manga M (2001) Origin of postseismic streamflow changes inferred from baseflow recession and magnitude-distance relation. *Geophys Res Lett* 28(10):2133–2136. <https://doi.org/10.1029/2000GL012481>
- Manga M, Rowland JC (2009) Response of Alum Rock springs to the October 30, 2007 Alum Rock earthquake and implications for the origin of increased discharge after earthquakes. *Geofluids* 9(3):237–250. <https://doi.org/10.1111/j.1468-8123.2009.00250.x>
- Manga M, Brodsky EE, Boone M (2003) Response of stream flow to multiple earthquakes. *Geophys Res Lett* 30(5):18–11
- Marchegiani L, Bertotti G, Cello G, Deiana G, Mazzoli S, Tondi E (1999) Pre-orogenic tectonics in the Umbria-Marche sector of the Afro-Adriatic continental margin. *Tectonophysics* 315(1–4):123–143. [https://doi.org/10.1016/S0040-1951\(99\)00277-2](https://doi.org/10.1016/S0040-1951(99)00277-2)
- Martarelli L, Petitta M, Scalise AR, Silvi A (2008) Experimental hydrogeological cartography of the Rieti plain (Latium). *Mem Descr Carta Geol d'It* 81:137–156
- Mastrorillo L, Petitta M (2014) Hydrogeological conceptual model of the upper Chienti River basin aquifers (Umbria-Marche Apennines). *Ital J Geosci* 133(3):396–408. <https://doi.org/10.3301/IJG.2014.12>
- Mastrorillo L, Baldoni T, Banzato F, Boscherini A, Cascone D, Checucci R, Petitta M, Boni C (2009) Quantitative hydrogeological analysis of the carbonate domain of the Umbria region (central Italy). *Ital J Eng Geol Environ* 1:137–155
- Mogi K, Mochizuki H, Kurokawa Y (1989) Temperature changes in an artesian spring at Usami in the Izu peninsula (Japan) and their relation to earthquakes. *Tectonophysics* 159(1–2):95–108. [https://doi.org/10.1016/0040-1951\(89\)90172-8](https://doi.org/10.1016/0040-1951(89)90172-8)
- Mohr CH, Manga M, Wang CY, Kirchner JW, Bronstert A (2015) Shaking water out of soil. *Geology* 43(3):207–210. <https://doi.org/10.1130/G36261.1>
- Mohr CH, Manga M, Wang CY, Korup O (2016) Regional changes in streamflow after a megathrust earthquake. *Earth Planet Sci Lett*. <https://doi.org/10.1016/j.epsl.2016.11.013>
- Montgomery DR, Manga M (2003) Streamflow and water well responses to earthquakes. *Science* 300(5628):2047–2049. <https://doi.org/10.1126/science.1082980>
- Montgomery DR, Greenberg HM, Smith DT (2003) Streamflow response to the Nisqually earthquake. *Earth Planet Sci Lett* 209(1–2):19–28. [https://doi.org/10.1016/S0012-821X\(03\)00074-8](https://doi.org/10.1016/S0012-821X(03)00074-8)
- Muir-Wood R, King GCP (1993) Hydrological signatures of earthquake strain. *J Geophys Res Solid Earth* 98:22035–22068. <https://doi.org/10.1029/93JB02219>
- Nanni T, Vivalda P (2005) The aquifers of the Umbria-Marche Adriatic region: relationships between structural setting and groundwater chemistry. *Boll Soc Geol It* 124:523–542
- Pantosti D, Valensise G (1990) Faulting mechanism and complexity of the November 23, 1980, Campania-Lucania earthquake, inferred from surface observations. *J Geophys Res* 95(B10):15,319–15,341. <https://doi.org/10.1029/JB095Ib10P15319>
- Parvin M, Tadakuma N, Asaue H, Koike K (2014) Delineation and interpretation of spatial coseismic response of groundwater levels in shallow and deep parts of an alluvial plain to different earthquakes: a case study of the Kumamoto Citi area, southwest Japan. *J Asian Earth Sci* 83:35–47. <https://doi.org/10.1016/j.jseas.2014.01.011>
- Petitta M (2009) Hydrogeology of the middle valley of the Velino River and of the S. Vittorino plain (Rieti, central Italy). *Ital J Eng Geol Environ* 1:157–182
- Petitta M, Tallini M (2002) Idrodinamica sotterranea del massiccio del Gran Sasso (Abruzzo): indagini idrologiche, idrogeologiche e idrochimiche 1994–2001 [Groundwater hydrodynamics of the Gran Sasso massif (Abruzzo): new hydrological, hydrogeological and hydrochemical surveys 1994–2001]. *Boll Soc Geol It* 121(3):343–363
- Petitta M, Primavera P, Tuccimei P, Aravena R (2011) Interaction between deep and shallow groundwater systems in areas affected by quaternary tectonics (central Italy): a geochemical and isotope

- approach. *Environ Earth Sci* 63(1):11–30. <https://doi.org/10.1007/s12665-010-0663-7>
- Pierantoni PP, Deiana G, Romano A, Paltrinieri W, Borraccini F, Mazzoli S (2005) Geometrie strutturali lungo la thrust zone del fronte montuoso Umbro-Marchigiano-Sabino [Structural geometries along the thrust zone of the Umbria-Marche-Sabina mountain front]. *Boll Soc Geol It* 124(2):395–411
- RCMT (2016) European-Mediterranean regional centroid-moment tensor catalog: <http://www.bo.ingv.it/RCMT/>. Accessed 5 Dec 2017
- Regione Marche (2017) SIRMIP ON-LINE - Marche Region - Civil Protection Service, Regional Meteorological-Hydrological Information System. <http://84.38.48.145/sol/indexjs.php?lang=en>. Accessed 3 Dec 2017
- Regione Umbria (2017) Dati Idrologici [Hydrological data]. <http://www.idrografico.regione.umbria.it/annali/>. Accessed 3 Dec 2017
- Rexin EE, Oliver J, Prentiss D (1962) Seismically-induced fluctuations of the water level in the Nunn-bush well in Milwaukee. *Bull Seism Soc Am* 52:17–25
- Roeloffs EA (1998) Persistent water level changes in a well near Parkfield, California, due to local and distant earthquakes. *J Geophys Res: Solid Earth* 103(1):869–889
- Roeloffs EA, Sneed M, Galloway DL, Sorey ML, Farrar CD, Howle JF, Hughes J (2003) Water-level changes induced by local and distant earthquakes at Long Valley Caldera California. *J Volcanol Geotherm Res* 127(3–4):269–303. [https://doi.org/10.1016/S0377-0273\(03\)00173-2](https://doi.org/10.1016/S0377-0273(03)00173-2)
- Rojstaczer S, Wolf S (1992) Permeability changes associated with large earthquakes: an example from Loma Prieta California. *Geology* 20(3):211–214. [https://doi.org/10.1130/0091-7613\(1992\)020<0211:PCAWLE>2.3.CO;2](https://doi.org/10.1130/0091-7613(1992)020<0211:PCAWLE>2.3.CO;2)
- Rojstaczer S, Wolf S, Michel R (1995) Permeability enhancement in the shallow crust as a cause of earthquake-induced hydrological changes. *Nature* 373(6511):237–239. <https://doi.org/10.1038/373237a0>
- Sato T, Sakai R, Furuya K, Kodama T (2000) Coseismic spring flow changes associated with the 1995 Kobe earthquake. *Geophys Res Lett* 27(8):1219–1222. <https://doi.org/10.1029/1999GL011187>
- Shi Z, Wang G, Manga M, Wang CY (2015) Continental-scale water-level response to a large earthquake. *Geofluids* 15(1–2):310–320. <https://doi.org/10.1111/gfl.12099>
- Sibson RH (1994) Crustal stress, faulting and fluid flow. *Geol Soc Spec Publ* 78:69–84. <https://doi.org/10.1144/GSL.SP.1994.078.01.07>
- Skelton A, Andrén M, Kristmannsdóttir H, Stockmann G, Mörth CM, Sveinbjörnsdóttir Á, Jónsson S, Sturkell E, Guðrúnardóttir HR, Hjartarson H, Siegmund H, Kockum I (2014) Changes in groundwater chemistry before two consecutive earthquakes in Iceland. *Nat Geosci* 7(10):752–756. <https://doi.org/10.1038/NGEO2250>
- Smeraglia L, Billi A, Carminati E, Cavallo A, Doglioni C (2017) Field- to nano-scale evidence for weakening mechanisms along the fault of the 2016 Amatrice and Norcia earthquakes, Italy. *Tectonophysics* 712–713:156–169. <https://doi.org/10.1016/j.tecto.2017.05.014>
- USGS (2017) Earthquake hazards program, <https://earthquake.usgs.gov/earthquakes/eventpage/usp0001zbv#executive>. Accessed 3 Dec 2017
- Wakita H (1975) Water wells as possible indicators of tectonic strain. *Science* 189(4202):553–555. <https://doi.org/10.1126/science.189.4202.553>
- Wang CY, Chia Y (2008) Mechanism of water level changes during earthquakes: near field versus intermediate field. *Geophys Res Lett* 35(12):L12402. <https://doi.org/10.1029/2008GL034227>
- Wang CY, Manga M (2010) Hydrologic responses to earthquakes and a general metric. *Geofluids* 10(1–2):206–216. <https://doi.org/10.1111/j.1468-8123.2009.00270.x>
- Wang CY, Manga M (2015) New streams and springs after the 2014 Mw6.0 South Napa earthquake. *Nat Commun* 6:7597. <https://doi.org/10.1038/ncomms8597>
- Wang CY, Wang CH, Kuo CH (2004a) Temporal change in groundwater level following the 1999 (mw 7.5) Chi-Chi earthquake, Taiwan. *Geofluids* 4(3):210–220. <https://doi.org/10.1111/j.1468-8123.2004.00082.x>
- Wang CY, Wang CH, Manga M (2004b) Coseismic release of water from mountains: evidence from the 1999 (mw=7.5) Chi-Chi, Taiwan, earthquake. *Geology* 32:769–772. <https://doi.org/10.1130/G20753.1>
- Wang CY, Wang LP, Manga M, Wang CH, Chen CH (2013) Basin-scale transport of heat and fluid induced by earthquakes. *Geophys Res Lett* 40(15):3893–3897. <https://doi.org/10.1002/grl.50738>
- Yan R, Woith H, Wang R (2014) Groundwater level changes induced by the 2011 Tohoku earthquake in China mainland. *Geophys J Int* 199(1):533–548. <https://doi.org/10.1093/gji/ggu196>